Interface transferring mechanism and error modification of FRP-OFBG strain sensors based on Findley's power law creep model

J.L. Li
School of Civil Engineering, Harbin Institute of Technology, Harbin, China
School of Astronautics, Harbin Institute of Technology, Harbin, China
Z. Zhou & J.P. Ou
School of Civil Engineering, Harbin Institute of Technology, Harbin, China

ABSTRACT: This paper presents the interface transferring mechanism and error modification of the Fiber Reinforced Polymer-Optical Fiber Bragg Grating (FRP-OFBG) sensing tendons, which including GFRP-OFBG (Glass Fiber Reinforced Polymer-Optical Fiber Bragg Grating) and CFRP-OFBG (Carbon Fiber Reinforced Polymer-Optical Fiber Bragg Grating), using Findley's power law creep model combining Boltzmann superposition principle. The optical fiber is made up of glass, quartz or plastic, et al, which creep strain are very small at room temperature. So the tensile creep compliance of optical fiber is independent of time at room temperature. On the other hand, the FRP (GFRP or CFRP) is composed of a polymeric matrix, for example epoxy resins, with glass or carbon fibers, which shear creep strains are dependent of time at room temperature. Hence, the Findley's power law model is employed to describe the creep compliance of FRP when linear viscoelastic behavior is assumed. The expression of interface strain transferring mechanism of FRP-OFBG sensors is derived based on linear viscoelastic theory. And the transient and steady-state error rate of FRP-OFBG sensors is obtained using initial value and final value theorems. Then a reformative initial value principle is given to describe the changing of the error rate following the loading time. Finally, an example is given to explain the correct of the new principle.

1 INTRODUCTION

Economic and life-safety issues have promoted significant research in the fields of structural health monitoring (SHM) and non-destructive evaluation in recent years. As a novel sensor, FRP-OFBG sensing tendon[1] has been applied in civil engineering structural health monitoring. This kind of sensor is composed of optical fiber Bragg grating and FRP tendon, and its strain monitoring error is less than 5% (Zhou2003, Li et al. 2004a, Zhou et al. 2003). The materials properties and dimension of FRP and OFBG will affect the interface strain transferring and error of FRP-OFBG sensors. The interface transferring properties of the fiber-optic sensors (including FRP-OFBG sensors) already brought correlative scholars to pay attention to this field, and some useful accomplishments have been gained. There are a lot of scholars, for example, Nanni (1991), Ansari (1998), Duck (1999), Lau (2001), Zhou et al (2002a,b) and Zhou (2003) do some significant works on this field. Li et al (2004a,b) presented the theoretical models and experiment researches on interface strain transferring mechanism and error modification of embedded and adhered FBG sensors. All researches are based on the linear elastic theory of material.

FRP reinforcement or tendons consist of aligned continuous fibers, mainly carbon (CFRP), glass (GFRP) or aramid (AFRP), embedded in a resin matrix such as epoxy, polyester, or vinyl ester by a pultrusion process. And OFBG sensors are embedded in the center of FRP tendons becoming FRP-OFBG sensing tendons. The strain of OFBG is independent of time but FRP tendon is a nonisotropic composite which strain subjected longtime loads is dependent of time at room temperature. Hence the creep characteristic of FRP tendon will affect the interface strain transferring laws of FRP-OFBG sensors. Kalamkarov et al (2000) characterized the long-term creep behavior of pultruded FRP tendons with the embedded fiber optic sensors, and their suitability for monitoring long-term service conditions. Patrick (2003) discusses the experimental results on properties and transfer length of the common types of fiber-reinforced polymer (FRP) tendons. Colin et al (2005) review the literature for information that is pertinent to creep in composite materials in order to develop a basic understanding of creep mechanisms and how

they pertain to a SHM paradigm. In general, creep along the fiber direction will be much less than shear induced or transverse creep due to the reinforcement of the fibers and is usually linear for temperatures that are much less than the glass transition temperature of the matrix and for time-invariant, low magnitude stress. And the matrix dominates creep, however, at long time scales creep begins to be dominated by the fibers if the load is parallel to the fiber direction. Obviously, the shear creep compliance along the fiber direction is one of the key factors to evaluate the interface strain transferring mechanism and error coefficient. But there is lack of literatures about shear creep compliance of aligned continuous fibers FRP tendons. Li et al (2005) have presented results of the theoretical part on creep behavior of FBG sensors.

It is evident from the previous research that Findley's power law creep model is adequate in describing the creep behavior of FRP composites. Findley's (1987) model was validated by long-term creep tests for tension, compression, and combined tension and torsion over a period of 26 years, and is recommended by the American Society of Civil Engineers (Task Committee ASCE 1984) in its Structural Plastics Design Manual. Because FRP-OFBG sensing tendons are linear viscoelastic structure, the Boltzmann superposition principle is practicable (Li et al. 2005).

This paper presents the interface transferring mechanism and error modification of FRP-OFBG sensors using Findley's power law creep model combining Boltzmann superposition principle. One hand, based on the linear viscoelastic constitutive relations, the expression of FRP-OFBG sensors interface strain transferring mechanism is derived, and the error-modified equation of FRP-OFBG sensors is obtained. And then, the transient and steady state responses of FRP-OFBG sensors are presented using initial value and final value theorems. At last, the future methods on this problem, for example, nonlinear vicoelastic model, micromechanics method et al, are prognosticated.

2 INTERFACE STRAIN TRANSFERRING MECHANISM

2.1 *Cylindrical model and displacement relationship*

Because the FRP-OFBG sensing tendon embedded in the host material is axial symmetry, circular cylindrical coordinates are shown in figure1, where x is the axial coordinate and r is radial coordinate, the symbols r_h and r_c represent the inner radius of the host material and the outer radii of the bare optical fiber, respectively measured from the centre of the optical fiber core, $2l_f$ is the effective working length of the FRP-OFBG sensors.

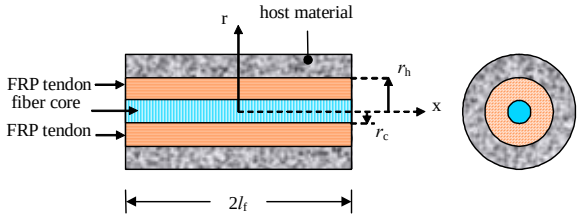

Figure 1 Cylindrical model of FRP-OFBG sensing tendon

The basic hypotheses:

1) The optical fiber and host material are linear viscoelasticity isotropic body, but FRP tendon is linear viscoelasticity nonisotropic body.

2) All of interfaces are continuous and satisfy the displacement compatibility.

3) Without regard to the temperature effect and considering the environment temperature is constant.

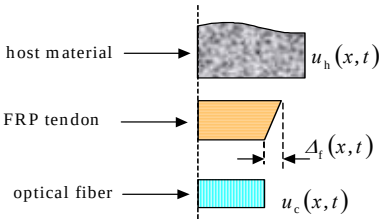

Figure 2 Relationship of deformation for cylindrical model

According to the hypotheses of displacement continuousness, there is a relative displacement between the optical fiber and the host material, which is resulted from the shear deformations of the FRP tendon. In figure 2 (for the axial symmetry, showing a quarter-cylinder model), the relationship of ever displacement is given by

$$u_h(x,t) = \Delta_f(x,t) + u_c(x,t) \tag{1}$$

Where the symbols $u_c(x,t)$ and $u_h(x,t)$ represent the displacement of optical fiber and host material respectively and $\Delta_f(x,t)$ is the relative displacement between optical fiber and host material, t is time. When x=0, the strains for all layers are mathematically identical, namely

$$\varepsilon_h(r,0,t) = \varepsilon_f(r,0,t) = \varepsilon_c(r,0,t) \tag{2}$$

2.2 *Balance equation for infinitesimal element*

(1) Balance equation of optical fiber infinitesimal element

For the optical fiber is insensitive to the transverse stresses (Li et al. 2004a), the effects of the transverse normal and shear stresses are ignored, and the lengthwise normal and shear stresses are

considered only. By considering the axial forces equilibrium for an element of the optical fiber at arbitrary point x, shown in figure 3, we can obtain an equation simplified as

$$\frac{\partial \sigma_c(x,t)}{\partial x} = -\frac{2\tau_{fc}(r_c,x,t)}{r_c} \tag{3}$$

where σ_c is tensile stress of optical fiber, τ_{fc} is the interface shear stress between the optical fiber and the FRP tendon.

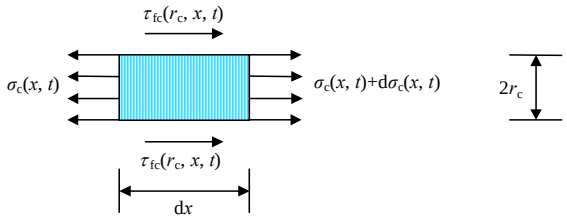

Figure 3 Infinitesimal element of optical fiber

(2) Balance equation for infinitesimal element of FRP tendon

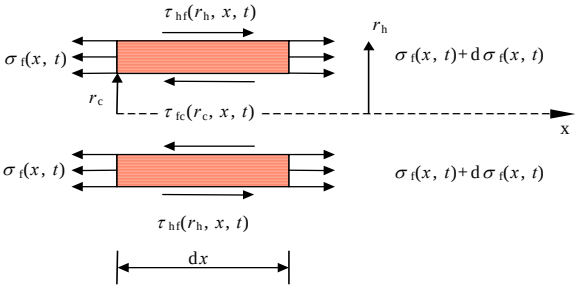

Figure 4 Infinitesimal element of FRP tendon

Figure 4 is the infinitesimal element of protective coating. According to the relationship of deformation compatibility, approximate expression (Christensen 1982) can be obtained by

$$\tau_f(r,x,t) = \frac{r_h}{r}\tau_{hf}(r_h,x,t) \qquad r_c \le r \le r_h \tag{4}$$

When $r = r_c$, there is

$$\tau_{fc}(r_c,x,t)\,r_c = \tau_{hf}(r_h,x,t)\,r_h \tag{5}$$

Considering the axial balance (x direction), $\frac{\partial \sigma_f(x,t)}{\partial x} = 0$, then

$$\sigma_f(x,t) = \sigma_f(t) \tag{6}$$

If the effective testing length of the optical fibre is a less, we can take for

$$\sigma_h(x,t) = \sigma_h(t) \tag{7}$$

2.3 *Stieltjes convolution integral creeping type constitutive equations and relationship between Displacement and Stress*

Because FRP tendon and host material are linear viscoelasticity, their constitutive relation can be written as Stieltjes convolution integral (Christensen 1982) based on Boltzmann superposition principle:

$$\begin{aligned}\varepsilon_h(x,t) &= J_h(t) * \mathrm{d}\sigma_h(x,t) \\ &= J_h(t)\sigma_h(x,0) + \int_0^t J_h(t-\tau)\frac{\partial \sigma_h(x,\tau)}{\partial \tau}\mathrm{d}\tau\end{aligned} \tag{8}$$

$$\begin{aligned}\varepsilon_c(x,t) &= J_c(t) * \mathrm{d}\sigma_c(x,t) \\ &= J_c(t)\sigma_c(x,0) + \int_0^t J_c(t-\tau)\frac{\partial \sigma_c(x,\tau)}{\partial \tau}\mathrm{d}\tau\end{aligned} \tag{9}$$

$$\begin{cases}\gamma_f(x,t) = J_f(t) * \mathrm{d}\tau(r,x,t) \\ \qquad = J_f(t)\tau_f(r,x,0) + \int_0^t J_f(t-\xi)\frac{\partial \tau_f(r,x,\xi)}{\partial \xi}\mathrm{d}\xi \\ r_c \le r \le r_h\end{cases} \tag{10}$$

Where $J_h(t)$ and $J_c(t)$ represent the tensile creep compliance of the host material and optical fiber core respectively, $J_f(t)$ represents the shear creep compliance of FRP tendon, and $\sigma_h(x, 0)$, $\sigma_c(x, 0)$ and $\tau_f(r, x, 0)$ represent the initial value of every layer material.

Considering above constitutive equations, the axial displacements of the host material and the optical fiber, the relative displacements of adhesive layer and protective coating are given by

$$\begin{aligned}u_h(x,t) &= \int_0^x \varepsilon_h(x,t)\mathrm{d}x = \int_0^x [J_h(t) * \mathrm{d}\sigma_h(x,t)]\mathrm{d}x \\ &= J_h(t) * \mathrm{d}\left[\int_0^x \sigma_h(x,t)\mathrm{d}x\right]\end{aligned} \tag{11}$$

$$\begin{aligned}u_c(x,t) &= \int_0^x \varepsilon_c(x,t)\mathrm{d}x = \int_0^x [J_c(t) * \mathrm{d}\sigma_c(x,t)]\mathrm{d}x \\ &= J_c(t) * \mathrm{d}\left[\int_0^x \sigma_c(x,t)\mathrm{d}x\right]\end{aligned} \tag{12}$$

$$\begin{aligned}\Delta_f(x) &= \int_{r_c}^{r_h} \gamma_f(r,x,t)\mathrm{d}r = \int_{r_c}^{r_h} [J_f(t) * \mathrm{d}\tau_f(r,x,t)]\mathrm{d}r \\ &= J_f(t) * \mathrm{d}\left[\int_{r_c}^{r_h} \tau_f(r,x,t)\mathrm{d}r\right]\end{aligned} \tag{13}$$

2.4 *Differential Equation and Solution*

(1) Differential equation

Substituting Eqs.(11), (12)and (13) into Eq. (1), making use of Eqs.(2) and (4), differentiated two times about x and noticing Eqs.(3), (5) and (7), we can obtain

$$\ln\left(\frac{r_h}{r_c}\right)J_f(t) * \mathrm{d}\left[\frac{\partial^2 \tau_{hf}(r_h,x,t)}{\partial x^2}\right] - \frac{2}{r_c^2}J_c(t) * \mathrm{d}\tau_{hf}(r_h,x,t) = 0 \tag{14}$$

We make Laplace transform on Eq. (17), and let

$$\bar{\lambda}^2 = \frac{2}{r_c^{\,2} \ln \frac{r_h}{r_c}} \cdot \frac{\bar{J}_c(s)}{\bar{J}_f(s)} \tag{15}$$

We can obtain differential equation as follows:

$$\frac{\partial^2 \bar{\tau}_{hf}(r_h, x, s)}{\partial x^2} - \bar{\lambda}^2 \bar{\tau}_{hf}(r_h, x, s) = 0 \tag{16}$$

Where $\bar{\tau}_{hf}(r_h, x, s)$, $\bar{J}_c(s)$ and $\bar{J}_f(s)$ represent Laplace transform couple of $\tau_{hf}(r_h, x, t)$, $J_c(t)$ and $J_f(t)$ respectively, $\bar{\lambda}$ is the eigenvalue of differential equation (16) but not the Laplace transform couple of λ.

(2) Solution

The complete solution to Eq. (16) is given by

$$\bar{\tau}_{hf}(r_h, x, s) = A(s)\cosh(\bar{\lambda}x) + B(s)\sinh(\bar{\lambda}x) \tag{17}$$

where $A(s)$ and $B(s)$ are integral constants decided by the boundary conditions.

The axes force of optical fiber can be written as follows

$$N_c(x,t) = \int_{A_c} \sigma_c(x,t)\mathrm{d}A \tag{18}$$

Integral Eq. (3), notice Eq. (5) and when x=0, $\sigma_c(0, t) = \sigma_c(t)$, then

$$\sigma_c(x,t) = \sigma_c(t) - \frac{2r_h}{r_c^2}\int_0^x \tau_{hf}(r_h, x, t)\mathrm{d}x \tag{19}$$

Substitute Eq. (19) into Eq. (18), we can obtain

$$N_c(x,t) = \pi r_c^2 \sigma_c(t) - 2\pi r_h \int_0^x \tau_{hf}(r_h, x, t)\mathrm{d}x \tag{20}$$

Making Laplace transform on Eqs. (19) and (20), then become

$$\bar{\sigma}_c(x,s) = \bar{\sigma}_c(s) - \frac{2r_h}{r_c^2}\int_0^x \bar{\tau}_{hf}(r_h, x, s)\mathrm{d}x \tag{21}$$

$$\bar{N}_c(x,s) = \pi r_c^2 \bar{\sigma}_c(s) - 2\pi r_h \int_0^x \bar{\tau}_{hf}(r_h, x, s)\mathrm{d}x \tag{22}$$

Substitute Eq. (17) into Eq. (22), there be

$$\bar{N}_c(x,s) = \pi r_c^2 \bar{\sigma}_c(s) - 2\pi r_h \frac{1}{\bar{\lambda}} \times \left[A(s)\sinh(\bar{\lambda}x) + B(s)\cosh(\bar{\lambda}x) + B(s)\right] \tag{23}$$

Considering Laplace transform of Eq. (2), $\bar{\varepsilon}_c(r_c, 0, s) = \bar{\varepsilon}_h(r_h, 0, s)$ and when $x = l_f$ the fibre-optic axial force is zero, then

$$\bar{N}_c(0,s) = \pi r_c^{\,2} \bar{\sigma}_c(s), \quad \bar{N}_c(l_f, s) = 0 \tag{24}$$

where l_f is the distance measured from the mid-beam (x = 0) to the point of zero axial load of the fibre. Using above boundary condition, the constants $A(s)$ and $B(s)$ are obtained by

$$A(s) = \frac{\bar{\sigma}_c(s) r_c^2 \bar{\lambda}}{2r_h \sinh(\bar{\lambda} l_f)}, \qquad B(s) = 0 \tag{25}$$

Combining Eqs. (17) and (25) yields the final form of shear stress distribution at the interface between the adhesive layer and protective coating in Laplace transform space

$$\bar{\tau}_{hf}(r_h, x, s) = \frac{\bar{\sigma}_c(s) r_c^2 \bar{\lambda}}{2r_h \sinh(\bar{\lambda} l_f)} \cosh(\bar{\lambda}x) \tag{26}$$

Substitute Eq. (26) into Eq. (21), there be

$$\bar{\sigma}_c(x,s) = \bar{\sigma}_c(s)\left[1 - \frac{\sinh(\bar{\lambda}\bar{x})}{\sinh(\bar{\lambda} l_f)}\right] \tag{27}$$

Considering the Laplace transform of Eq. (9)

$$\begin{cases} \bar{\varepsilon}_c(x,s) = \bar{J}_c(s) s \bar{\sigma}_c(x,s) \\ \bar{\varepsilon}_c(0,s) = \bar{J}_c(s) s \bar{\sigma}_c(0,s) \end{cases} \tag{28}$$

Substitute Eq. (27) into Eq. $(28)_1$ and notice $(28)_2$, We can obtain

$$\bar{\varepsilon}_c(x,s) = \bar{\varepsilon}_c(0,s)\left[1 - \frac{\sinh(\bar{\lambda}x)}{\sinh(\bar{\lambda} l_f)}\right] \tag{29a}$$

Considering the Laplace transform of Eqs. (2), (8) and (9), then

$$\begin{cases} \bar{\varepsilon}_c(0,s) = \bar{\varepsilon}_h(0,s) \\ \bar{\varepsilon}_h(x,s) = \bar{J}_h(s) s \bar{\sigma}_h(x,s) \\ \bar{\varepsilon}_h(0,s) = \bar{J}_h(s) s \bar{\sigma}_h(0,s) \end{cases} \tag{30}$$

Eq. (29a) can be written as follows:

$$\bar{\varepsilon}_c(x,s) = \bar{\varepsilon}_h(0,s)\left[1 - \frac{\sinh(\bar{\lambda}x)}{\sinh(\bar{\lambda} l_f)}\right] \tag{29b}$$

Meanwhile,

$$\bar{\varepsilon}_c(x,s) = \bar{\sigma}_c(0,s)\bar{J}_c(s) s\left[1 - \frac{\sinh(\bar{\lambda}x)}{\sinh(\bar{\lambda} l_f)}\right] \tag{29c}$$

$$\bar{\varepsilon}_c(x,s) = \bar{\sigma}_h(0,s)\bar{J}_h(s) s\left[1 - \frac{\sinh(\bar{\lambda}x)}{\sinh(\bar{\lambda} l_f)}\right] \tag{29d}$$

Making inverse Laplace transform on Eqs. (29), the interface strain transferring function of FRP-OFBG sensors can be presented as follows:

$$\varepsilon_c(x,t) = \Lambda^{-1}\left\{\bar{\varepsilon}_c(0,s)\left[1 - \frac{\sinh(\bar{\lambda}x)}{\sinh(\bar{\lambda} l_f)}\right]\right\} \tag{30a}$$

$$\varepsilon_c(x,t) = \Lambda^{-1}\left\{\bar{\varepsilon}_h(0,s)\left[1 - \frac{\sinh(\bar{\lambda}x)}{\sinh(\bar{\lambda} l_f)}\right]\right\} \tag{30b}$$

$$\varepsilon_{\mathrm{c}}(x,t)=\boldsymbol{\Lambda}^{-1}\left\{\overline{\sigma}_{\mathrm{c}}(0,s)\overline{J}_{\mathrm{c}}(s)s\left[1-\frac{\sinh(\overline{\lambda}x)}{\sinh(\overline{\lambda}l_{\mathrm{f}})}\right]\right\} \quad (30c)$$

$$\varepsilon_{\mathrm{c}}(x,t)=\boldsymbol{\Lambda}^{-1}\left\{\overline{\sigma}_{\mathrm{h}}(0,s)\overline{J}_{\mathrm{h}}(s)s\left[1-\frac{\sinh(\overline{\lambda}x)}{\sinh(\overline{\lambda}l_{\mathrm{f}})}\right]\right\} \quad (30d)$$

Given the shear creep compliance $J_{\mathrm{f}}(t)$ of FBG and tensile creep compliance $J_{\mathrm{c}}(t)$ of optical fiber, the $\overline{J}_{\mathrm{f}}(s)$ and $\overline{J}_{\mathrm{c}}(s)$ can be obtained and $\overline{\lambda}$ can be known too, then the strain of FRP-OFBG sensors at point x can be calculated by Eqs. (30).

3 CREEP CHARACTERISTIC ANALYSES AND AVERAGE CREEP STRAIN

3.1 *Creep test analyses*

If a step stress function at the point x=0 of fiber core host material is given as

$$\sigma_{\mathrm{c}}(0,t)=\sigma_{\mathrm{c}}H(t) \quad \sigma_{\mathrm{h}}(0,t)=\sigma_{\mathrm{h}}H(t) \quad (31)$$

where σ_{c} and σ_{h} are constant stress and $H(t)$ is Heaviside function, namely

$$H(t)=\begin{cases}0 & t<0\\ 1 & t>0\end{cases} \quad (32)$$

The Laplace transform couple of Eq. (31) is written as follows:

$$\overline{\sigma}_{\mathrm{c}}(0,s)=\frac{\sigma_{\mathrm{c}}}{s} \quad \overline{\sigma}_{\mathrm{h}}(0,s)=\frac{\sigma_{\mathrm{h}}}{s} \quad (33)$$

Institute Eq. (33) into Eq. (30c, d), then

$$\overline{\varepsilon}_{\mathrm{c}}(x,s)=\sigma_{\mathrm{c}}\overline{J}_{\mathrm{c}}(s)\left[1-\frac{\sinh(\overline{\lambda}x)}{\sinh(\overline{\lambda}l_{\mathrm{f}})}\right] \quad (34)$$

$$\overline{\varepsilon}_{\mathrm{c}}(x,s)=\sigma_{\mathrm{h}}\overline{J}_{\mathrm{h}}(s)\left[1-\frac{\sinh(\overline{\lambda}x)}{\sinh(\overline{\lambda}l_{\mathrm{f}})}\right] \quad (35)$$

The results of inverse Laplace transforms about Eqs. (34), (35) are follows:

$$\varepsilon_{\mathrm{c}}(x,t)=\sigma_{\mathrm{c}}\boldsymbol{\Lambda}^{-1}\left\{\overline{J}_{\mathrm{c}}(s)\left[1-\frac{\sinh(\overline{\lambda}x)}{\sinh(\overline{\lambda}l_{\mathrm{f}})}\right]\right\} \quad (36)$$

$$\varepsilon_{\mathrm{c}}(x,t)=\sigma_{\mathrm{h}}\boldsymbol{\Lambda}^{-1}\left\{\overline{J}_{\mathrm{h}}(s)\left[1-\frac{\sinh(\overline{\lambda}x)}{\sinh(\overline{\lambda}l_{\mathrm{f}})}\right]\right\} \quad (37)$$

If a step strain function at the point x=0 of fiber core and host material is given as

$$\varepsilon_{\mathrm{c}}(0,t)=\varepsilon_{\mathrm{c}}H(t) \quad \varepsilon_{\mathrm{h}}(0,t)=\varepsilon_{\mathrm{h}}H(t) \quad (38)$$

$$\overline{\varepsilon}_{\mathrm{c}}(0,s)=\frac{\varepsilon_{\mathrm{c}}}{s} \quad \overline{\varepsilon}_{\mathrm{h}}(0,s)=\frac{\varepsilon_{\mathrm{h}}}{s} \quad (39)$$

Similar to the above, institute Eq. (39) into Eq. (30a, d), then

$$\varepsilon_{\mathrm{c}}(x,t)=\varepsilon_{\mathrm{c}}\boldsymbol{\Lambda}^{-1}\left\{\frac{1}{s}\cdot\left[1-\frac{\sinh(\overline{\lambda}x)}{\sinh(\overline{\lambda}l_{\mathrm{f}})}\right]\right\} \quad (40)$$

$$\varepsilon_{\mathrm{c}}(x,t)=\varepsilon_{\mathrm{h}}\boldsymbol{\Lambda}^{-1}\left\{\frac{1}{s}\cdot\left[1-\frac{\sinh(\overline{\lambda}x)}{\sinh(\overline{\lambda}l_{\mathrm{f}})}\right]\right\} \quad (41)$$

3.2 *Average creep strain*

From Eq. (41), it is clearly that there is difference at the testing point between the axial strain of the optical fibre ($\varepsilon_{\mathrm{c}}(x, t)$) and the host material ($\varepsilon_{\mathrm{h}}(x, t)$). If and only if x=0, then $\varepsilon_{\mathrm{c}}(0, t)=\varepsilon_{\mathrm{h}}(0, t)$. While monitoring, we could not obtain the strain of every point of x where the FRP-OFBG sensor is set up. Hence, in order to estimate the error between the testing strain of the FRP-OFBG sensor and the practical strain of the host material and modify it, the average measured strain of FRP-OFBG sensor and the host material are defined as

$$\boldsymbol{\epsilon}_{\mathrm{c}}(t)=\frac{\int_0^{l_{\mathrm{f}}}\varepsilon_{\mathrm{c}}(x,t)\mathrm{d}x}{l_{\mathrm{f}}}, \quad \boldsymbol{\epsilon}_{\mathrm{h}}(t)=\frac{\int_0^{l_{\mathrm{f}}}\varepsilon_{\mathrm{h}}(x,t)\mathrm{d}x}{l_{\mathrm{f}}} \quad (42)$$

If l_{f} is small value, let $\varepsilon_{\mathrm{h}}(x, t)=\varepsilon_{\mathrm{h}}(0, t)=\varepsilon_{\mathrm{h}}H(t)$, then the average strains are

$$\boldsymbol{\epsilon}_{\mathrm{h}}(t)=\varepsilon_{\mathrm{h}}H(t) \quad (43)$$

$$\boldsymbol{\epsilon}_{\mathrm{c}}(t)=\varepsilon_{\mathrm{h}}\left(H(t)-\boldsymbol{\Lambda}^{-1}\left[\frac{\cosh(\overline{\lambda}l_{\mathrm{f}})-1}{s\overline{\lambda}l_{\mathrm{f}}\sinh(\overline{\lambda}l_{\mathrm{f}})}\right]\right) \quad (44)$$

We define the creep strain transferring error rate $\eta(t)$ and the creep strain modified coefficient $k(t)$ as follows:

$$\eta(t)=\frac{|\boldsymbol{\epsilon}_{\mathrm{c}}(t)-\boldsymbol{\epsilon}_{\mathrm{h}}(t)|}{\boldsymbol{\epsilon}_{\mathrm{h}}(t)}=\boldsymbol{\Lambda}^{-1}\left[\frac{\cosh(\overline{\lambda}l_{\mathrm{f}})-1}{s\overline{\lambda}l_{\mathrm{f}}\sinh(\overline{\lambda}l_{\mathrm{f}})}\right] \quad (45)$$

$$k(t)=\frac{1}{1-\eta(t)} \quad (46)$$

then

$$\boldsymbol{\epsilon}_{\mathrm{h}}(t)=k(t)\boldsymbol{\epsilon}_{\mathrm{c}}(t) \quad (47)$$

This equation gives the relationship between the FRP-OFBG sensor testing creep strain and the practical strain of the host material, as well as affords the theory base for the creep analysis and modification of the system error.

4 FINDLEY'S POWER LAW AND IMAGE FUNCTION OF ERROR RATE η

4.1 *Findley's power law*

Many mathematical models have been proposed to describe the creep behavior of plastics in term of stress, strain, and time. Findley's power law has

become the most commonly used empirical to analyze the viscoelastic behavior of plastics and composites under constant stress because of its simplicity and successful simulation. Shao (2004), McClure (1995), and Scott (1998) respectively study tensile, shear, compressiom, and deflection creep of pultruded composite sheet piling, stub, and beam using Findley's power law model. The expression of Findley's model can be generalized to include different types of creep (Shao 2004). Inorder to discribe the shear creep compliance of FRP tendon, the shear creep strain is considered only

$$\gamma(t)=\gamma_0+m\left(\frac{t}{t_0}\right)^n \tag{48}$$

where $\gamma(t)$ is time-dependent shear creep strain, γ_0 is stress-dependent and time-independent initial shear strain, m is stress- and time-dependent shear creep coefficient, $0<n<1$ is stress-independent material constant for shear creep, t is time (hours), and t_0 is unit time (1 hour).

According to Shao (2004), the exact Findley's expression with hyperbolic sine functions and the simplified Findley's expression with linear relation differed by at most 4% after 75 years (Scott 1998). Therefore, within the primary and secondary creep regions, the linear vicoelastic behavior of composites could be assumed and the time-dependent viscoelastic shear modulus $G_f(t)$ could be calculated using Eq. (48):

$$G_f(t)=\frac{\tau_0}{\gamma(t)}=\frac{G_0\gamma_0}{\gamma_0+m\left(\frac{t}{t_0}\right)^n}=\frac{G_0G_t}{G_t+G_0\left(\frac{t}{t_0}\right)^n} \tag{49}$$

where τ_0, γ_0, and G_0 are time-independent intial shear stress, initial shear strain, and shear modulus, respestively. And $G_t=\tau_0/m=G_0\gamma_0/m$ is viscoelastic shear parameter.

Since Eq. (49) is derived from the simplified Findley's expression, the viscoelastic shear modulus $G_f(t)$ is independent of the stress lever and the viscoelastic shear parameter G_t should be a constant for a given material. It is indicative that the ratio of γ_0/m is close to a constant at different load lever. To apply Findley's model, coefficients m and material constant n in Eqs. (48) (49) have to be determined through curve fitting of experimental data. Rearranging Eq. (48) and taking the ln on both sides of equation gives

$$\ln[\gamma(t)-\gamma_0]=\ln(m)+n\ln\left(\frac{t}{t_0}\right) \tag{50}$$

When the logarithmic creep is plotted versus the logarithmic time, it is straight line, of which the slope yields the material constant n, and the y intercepts gives the value of ln(m).

4.2 *Image function of error rate* η

According to Eq. (49), the shear creep compliance of FRP tendon under the constant stress can be obtained as follow:

$$J_f(t)=\frac{\gamma(t)}{\tau_0}=\frac{1}{G_0}+\frac{1}{G_t}\cdot\left(\frac{t}{t_0}\right)^n \tag{51}$$

Because the optical fiber is made up of glass, which tensile creep strain is very small and can be ignored, the optical fiber can be adopted Hooke body. Then the tensile creep compliance is a constant, namely

$$J_c(t)=\frac{1}{E_c} \tag{52}$$

where E_c is the Young's modulus of the optical fiber.

The Laplace transform couple of Eqs. (51) (52) are written as follows:

$$\bar{J}_f(s)=\frac{1}{G_0}\cdot\frac{1}{s}+\frac{\Gamma(n+1)}{G_t t_0^n}\cdot\frac{1}{s^{n+1}} \tag{53}$$

$$\bar{J}_c(s)=\frac{1}{E_c}\cdot\frac{1}{s} \tag{54}$$

Substitute Eqs. (51) (52) into the Eq. (15), there be

$$\begin{aligned}\bar{\lambda}^2&=\frac{2G_0}{E_c r_c^2\ln\frac{r_h}{r_c}}\cdot\left(1+\frac{\Gamma(n+1)}{t_0^n}\cdot\frac{G_0}{G_t}\cdot s^{-n}\right)^{-1}\\&=\lambda_0^2\left(1+\frac{\Gamma(n+1)}{t_0^n}\cdot\frac{G_0}{G_t}\cdot s^{-n}\right)^{-1}\end{aligned} \tag{55}$$

where λ_0 is the initial eigenvalue of the equation (14), namely, the λ of equation (32) in the reference LI et al. 2004.

Let $a=\frac{\Gamma(n+1)}{t_0^n}\cdot\frac{G_0}{G_t}$, then Eq. (55) can be written

$$\bar{\lambda}=\lambda_0\left(1+as^{-n}\right)^{-\frac{1}{2}} \tag{56}$$

Let $z(s)=\bar{\lambda}l_f$, As a result, the image function of the error rate η can be expressed as:

$$\bar{\eta}(s)=\bar{\eta}[z(s)]=\frac{\cosh(z)-1}{sz\sinh(z)} \tag{57}$$

5 TRANSIENT AND STEADY-STATE RESPONSES OF ERROR RATE η

It is usually difficult to obtain an analytic expression from an inverse Laplace transform of Eq. (57). In order to research the creep responses of viscoelastic body, we usually adopt approximative solution. For example, numerical method analysis is to spread the $\overline{\eta}(s)$ as perpendicular function and then put up inverse Laplace transform. Another approximative solution is by the use of the initial and final value theorems of Laplace transform to find the transient and steady-state responses and then evaluate the creep influence.

5.1 *Transient response*

Noticing Eq. (56), we have:

$$\lim_{s\to\infty}\overline{\lambda}=\lim_{s\to\infty}\lambda_0\left(1+as^{-n}\right)^{-\frac{1}{2}}=\lambda_0 \tag{58}$$

$$\lim_{s\to\infty}z(s)=\lambda_0 l_{\mathrm{f}} \tag{59}$$

According to the initial theorem, the initial error rate $\eta(0)$, when t=0, can be obtained:

$$\begin{aligned}\eta(0)&=\lim_{t\to 0}\eta(t)=\lim_{s\to\infty}s\overline{\eta}(s)\\&=\lim_{s\to\infty}s\cdot\frac{\cosh(z(s))-1}{s\cdot z\sinh(z(s))}=\frac{\cosh(\lambda_0 l_{\mathrm{f}})-1}{\lambda_0 l_{\mathrm{f}}\sinh(\lambda_0 l_{\mathrm{f}})}\end{aligned} \tag{60}$$

This equation is same as the Eq. (28) of reference Li et al. 2004a, which present that the solution of elasticity is the transient responses of viscoelasticity.

5.2 *Steady-state response*

The same as 5.1, we can obtain steady-state solution as follows:

$$\lim_{s\to 0}\overline{\lambda}=\lim_{s\to 0}\lambda_0\left(1+as^{-n}\right)^{-\frac{1}{2}}=0 \tag{61}$$

$$\lim_{s\to 0}z(s)=\lim_{s\to 0}\overline{\lambda}l_{\mathrm{f}}=0 \tag{62}$$

According to the final theorem, when $t\to\infty$, noticing Eq. (62) and using L'Hospital principle, the final error rate $\eta(\infty)$ can be obtained:

$$\begin{aligned}\eta(\infty)&=\lim_{t\to\infty}\eta(t)=\lim_{s\to 0}s\eta(s)=\lim_{z\to 0}\frac{\cosh(z)-1}{z\sinh(z)}\\&=\lim_{z\to 0}\frac{\sinh(z)}{\sinh(z)+z\cosh(z)}\\&=\lim_{z\to 0}\frac{\cosh(z)}{2\cosh(z)+z\sinh(z)}=\frac{1}{2}\end{aligned} \tag{63}$$

Then, the initial and final values of the modification coefficient k can be obtained:

$$k(0)=\frac{1}{1-\eta(0)} \tag{64}$$

$$k(\infty)=\frac{1}{1-\eta(\infty)}=2 \tag{65}$$

In general, the extent of the error rate is between $\eta(0)$ and 1/2, namely:

$$\eta(0)\le\eta\le\eta(\infty)=1/2 \tag{66}$$

6 A NEW APPROXIMATIVE SOLUTION

Usually, the lifetime of FRP-OFBG is more than 50 years and less than 100 years. In engineering practice, the error rate of a certain time, for example 30 years or 60 years, is paid more attention to, whereas, couldn't be obtained from the method of the above. In order to calculate the error rate of a certain time, a new approximative method is given later.

6.1 *Reformative initial value principle*

Considering the characteristic of the initial value principle, that the initial value is independent of subsequence time, a reformative initial value principle is put foreword as followed:

Firstly, according to Eqs. (51) and (52), when $t=\tau$, the shear creep compliance of FRP and tensile creep compliance optical fiber can be written respectively:

$$J_{\mathrm{f}}(\tau)=\frac{1}{G_0}+\frac{1}{G_t}\cdot\left(\frac{\tau}{t_0}\right)^n \tag{67}$$

$$J_{\mathrm{c}}(\tau)=\frac{1}{E_{\mathrm{c}}} \tag{68}$$

Secondly, supposing that materials are solidified at the moment of τ and unloaded, at that time a new kind of materials are obtained, which initial creep compliances are $J_{\mathrm{f}}(\tau)$and $J_{\mathrm{c}}(\tau)$. And then, the creep compliances of the new kind of materials can be defined as:

$$\tilde{J}_{\mathrm{f}}(t)=J_{\mathrm{f}}(\tau)+\frac{1}{G_\tau}\cdot\left(\frac{t}{t_0}\right)^n \tag{69}$$

$$\tilde{J}_{\mathrm{c}}(t)=\frac{1}{E_{\mathrm{c}}} \tag{70}$$

where G_τ is dependent of τ, which calculating method is the same as G_t. Obviously, the value of Eq. (69) is bigger than the value of Eq. (51) in the same time extent. But the later calculation couldn't be affected.

Finally, repeating steps from Eq. (53) to (60), the main results can be expressed;

$$\bar{\tilde{J}}_{\mathrm{f}}(s)=J_{\mathrm{f}}(\tau)\frac{1}{s}+\frac{\Gamma(n+1)}{G_\tau t_0^n}\cdot\frac{1}{s^{n+1}} \tag{71}$$

$$\bar{\bar{J}}_c(s)=\frac{1}{E_c}\cdot\frac{1}{s} \tag{72}$$

$$\bar{\bar{\lambda}}^2=\frac{2}{J_f(\tau)E_c r_c^2\ln\frac{r_h}{r_c}}\cdot\left(1+\frac{\Gamma(n+1)}{t_0^n}\cdot\frac{1}{J_f(\tau)G_\tau}\cdot s^{-n}\right)^{-1}$$
$$=\lambda_\tau^2\left(1+a_\tau s^{-n}\right)^{-1} \tag{73}$$

$$\lambda_\tau=\sqrt{\frac{2}{J_f(\tau)E_c r_c^2\ln\frac{r_h}{r_c}}} \tag{74}$$

$$a_\tau=\frac{\Gamma(n+1)}{t_0^n}\cdot\frac{1}{J_f(\tau)G_\tau} \tag{75}$$

$$\bar{\bar{\lambda}}=\lambda_\tau\left(1+a_\tau s^{-n}\right)^{-\frac{1}{2}} \tag{76}$$

$$\tilde{z}(s)=\bar{\bar{\lambda}}l_f \tag{77}$$

$$\bar{\bar{\eta}}(s)=\bar{\bar{\eta}}[\tilde{z}(s)]=\frac{\cosh(\tilde{z})-1}{s\tilde{z}\sinh(\tilde{z})} \tag{78}$$

$$\lim_{s\to\infty}\tilde{z}(s)=\lim_{s\to\infty}\bar{\bar{\lambda}}l_f$$
$$=\lim_{s\to\infty}\lambda_\tau\left(1+a_\tau s^{-n}\right)^{-\frac{1}{2}}l_f=\lambda_\tau l_f=\tilde{z}(\tau) \tag{79}$$

$$\eta(\tau)=\tilde{\eta}(0)=\lim_{t\to0}\tilde{\eta}(t)=\lim_{s\to\infty}s\bar{\bar{\eta}}(s)$$
$$=\lim_{s\to\infty}s\cdot\frac{\cosh(\tilde{z}(s))-1}{s\cdot\tilde{z}\sinh(\tilde{z}(s))}=\frac{\cosh(\lambda_\tau l_f)-1}{\lambda_\tau l_f\sinh(\lambda_\tau l_f)} \tag{80}$$
$$=\frac{\cosh[\tilde{z}(\tau)]-1}{\tilde{z}(\tau)\sinh[\tilde{z}(\tau)]}$$

Obviously, given a creep time τ, the corresponding error rate $\eta(\tau)$ can be calculated from Eq. (80). And considering Eqs. (67), (74), (79) and (80), we will obtain some expressions as followed:

$$J_f(0)=\frac{1}{G_0},\quad J_c(0)=\frac{1}{E_c},\quad \tau=0 \tag{81}$$

then

$$\tilde{z}(0)=\lambda_\tau(0)l_f=\lambda_0 l_f \tag{82}$$

$$\eta(\tau)\big|_{\tau=0}=\frac{\cosh(\lambda_0 l_f)-1}{\lambda_0 l_f\sinh(\lambda_0 l_f)}=\eta(0) \tag{83}$$

When $\tau\to\infty$, there is $J_f(\infty)\to\infty$, and then $\lambda_\tau\to0$ and $\tilde{z}(\infty)\to0$, hence, using L'Hospital principle we have:

$$\eta(\tau)\big|_{\tau=\infty}=\lim_{\tau\to\infty}\eta(\tau)=\lim_{\tilde{z}\to0}\frac{\cosh\tilde{z}-1}{\tilde{z}\sinh\tilde{z}}=\frac{1}{2}=\eta(\infty) \tag{84}$$

then

$$\eta(0)\le\eta(\tau)\le\eta(\infty)=\frac{1}{2} \tag{85}$$

In general, not only is the same as between the Eqs. (85) and (66) in the form, but could be calculated the error rate at any time by the former.

6.2 *Calculating example*

For lack of the shear compliance experimental data of the GFRP tendon at hand, the experimental data G_0, G_t, and n come from Shao (2004). The other data come from Zhou (2003). All the data are summarized in Table 1.

Table 1 GFRP-OFBG Sensing Tendon Parameters

L_f(mm)	r_c(mm)	r_h(mm)	E_c(GPa)	G_0(GPa)	G_t(GPa)	n
10	6.25×10^{-2}	3,5,10	70	3.07	107	0.33

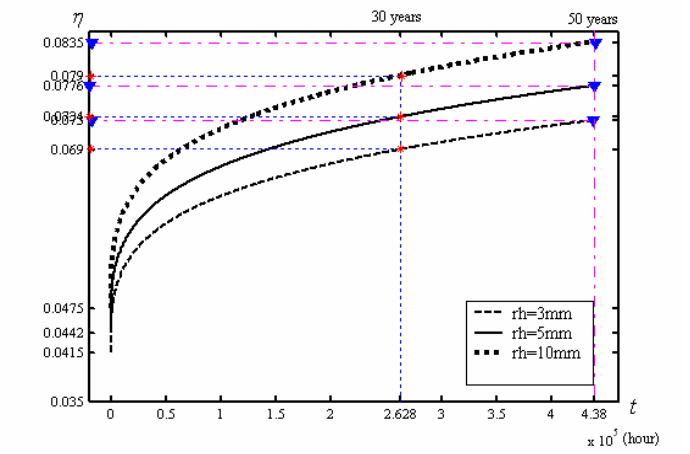

Figure 5 Creep error rate curves of GFRP-OFBG sensor

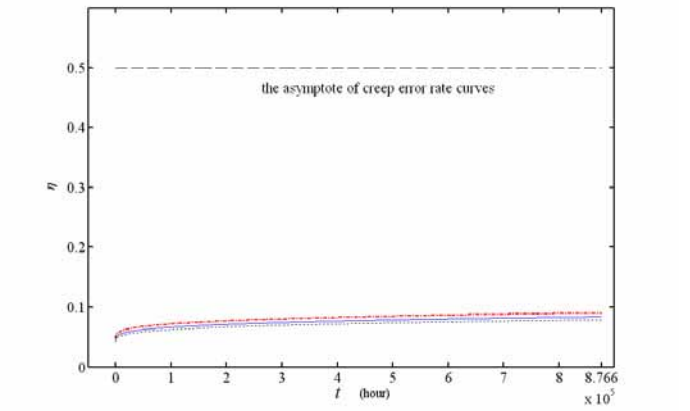

Figure 6 Creep error rate curves of GFRP-OFBG in 100 years

Substituting Eq. (67) into Eq. (80), using data of Table 1, we can calculate the error rate η at any time. Figure 5 gives the comparing curves about three sizes of GFRP-OFBG sensing tendons error

rate changing extent in 50 years, the rh is r_h, namely, the radius of the FRP tendon. In figure6, the three curves of GFRP-OFBG sensing tendons error rates in 100 years are compared to the steady response curve.

Results are stated that the type error rate creep curves of the GFRP-OFBG sensors are the same as the creep curves of the FRP materials. There is an initial value that is fully elastic followed by stage II or primary error rate induced creep, which is characterized a continuously decreasing error rate variation. Stage II (secondary or steady-state) error rate exhibits a constant variation of error rate. But not followed by stage III where the error rate variation increases rapidly until creep rupture because the Findley's power law model ignores the stage III creep of FRP materials. Comparing to the initial and final principle solution, this new approximative method can calculate the value of error rate at any time.

For example, when r_h=3mm, the error rate calculating data from Eq. (80) of the FRP-OFBG sensing tendon are displayed in table 2. Obviously, the fist 0.01 increment of error rate is in a period of 7152h(10m), and the second is in a period of 78840h(9years), the third is in a period of 359160h(41years). In a word, if the using time of FRP-OFBG sensors is less than 50 years, the increment of the error rate is 0.02 during the fist decade, and in the followed decades the increment of error rate is less than 0.01. Hence, convenient for using, the error rate is equaled average 0.0468 in the first year, and 0.0571 between 1th and 10^{th} year, and 0.0676 between 11^{th} and 50^{th} year.

Table 2 Error rates of FRP-OFBG sensors (r_h=3mm, r_h=rh)

τ(h)	0	7152	8760	78840	17520	262800	359160	438000	876600
d.m.y.	0	10m	1y	9y	20y	30y	41y	50y	100y
η(%)	0.0415	0.0515	0.0521	0.0614	0.0662	0.0690	0.0714	0.0730	0.0790

7 CONCLUSION

This paper presents the interface transferring mechanism and error modification of the FRP-OFBG sensing tendons using Findley's power law creep model combining Boltzmann superposition principle. The tensile creep compliance of optical fiber is independent of time at room temperature. And the shear creep strains of FRP (GFRP or CFRP) are dependent of time at room temperature. Hence, the Findley's power law model is employed to describe the creep compliance of FRP when linear viscoelastic behavior is assumed. The expression of interface strain transferring mechanism of FRP-OFBG sensors is derived based on linear viscoelastic theory. And the transient and steady-state error rate of FRP-OFBG sensors is obtained using initial value and final value theorems. Then a reformative initial value principle is given to describe the changing of the error rate following the loading time. At last, an example is given to explain the correct of the new principle.

Researches indicate that:

(1) The type error rate creep curves of the GFRP-OFBG sensors are the same as the creep curves of the FRP materials. There is an initial value that is fully elastic followed by stage II or primary error rate induced creep, which is characterized a continuously decreasing error rate variation. Stage II (secondary or steady - state) error rate exhibits a constant variation of error rate. But not followed by stage III where the error rate variation increases rapidly until creep rupture because the Findley's power law model ignores the stage III creep of FRP materials.

(2) If the using time of FRP-OFBG sensors is less than 50 years, the increment of the error rate is 0.02 during the fist decade, and in the followed decades the increment of error rate is less than 0.01. Hence, convenient for using, the error rate is equaled average 0.0468 in the first year, and 0.0571 between 1st and 10^{th} year, and 0.0676 between 11^{th} and 50^{th} year.

(3) Although it is difficult to obtain the analytical solution, the transient and steady-state responses is a very effective method for us to observe and learn the changing result of strain of FBG sensors influenced by creep of multiple layers interface material. Comparing to the initial and final principle solution, this new approximative method can calculate the value of error rate at any time.

(4) In order to verify the validity of above theories, a lot of experiments should be done in following researches.

(5) It is necessary to research this problem applied other principles which more accurate than Findley's model.

8 ACKNOWLEDGEMENT

This paper is supported by the National"863" High-Tech. research project (No.2001AA602023), National Natural Science Foundation of China (50308008) and China Postdoctoral Science Foundation.

9 REFERENCES

Ansari, F. & Yuan, L. 1998. Mechanics of bond and interface shear transfer in optical fibre sensors. *Journal Engineering Mechanics* 124(4): 385-394.

Christensen, R M. 1982. *Theory of Viscoelaticity, an Introduction*. Second edition, Academic Press, Inc.

Colin, O. Tim, F. & Micheal, T. 2005. A Literature-Based Summary Review of Creep Mechanism in Composite Materials: Key Parameters, Failure Modeling, and Environmental Effects. *UCSD/Los Alamos National Laboratory Graduate Education Initiative Phase I, Task 3: UCSD/LANL Collaborative Study in Monitoring Integrity of Composite Structural Joints.* www.jacobsschool.ucsd.edu/EEI/projects/pdf/LANL_Phase1_Task3_1.pdf.

Duck, G. Renaund, G. & Measures, M. 1999. The mechanical load transfer into a distributed optical fibre sensor due to a linear strain gradient: embedded and surface bonded case. *Journal Smart Materials Structure* 8: 175-181.

Findley, W. N. 1987. 26-year Creep and Recovery of Poly (Viny1 Chloride) and Polyethylene. *Polymer Engineering Science* 27(8): 582-585.

Kalamkarov, A. L. MacDonald, D. O. Fitzgerald, S. B. & Georgiades, A. V. 2000. Reliability assessment of pultruded FRP reinforcements with embedded fiber optic sensors. *Composites Structures* 50: 69-78.

Lau, K. Yuan, L. Zhou, L. et al. 2001. Strain monitoring in FRP laminates and concrete beams using FBG sensors. *Composite Structures* 51: 9-20.

Li, Jilong. Zhou, Zhi & Ou, Jinping. 2004a. Interface Transferring Mechanism and Error Modification of Embedded FBG Strain Sensor. *SPIE International Symposium Smart Structures and Materials, 14-18 March 2004. San Diego, California USA*. *Proc. SPIE Vol. 5384. Smart Structures and Materials: Smart Sensor Technology and Measurement Systems, Eric Udd, Daniele Inaudi; Eds.* Publication Date: Jul 2004: 190-198.

Li, Jilong. Zhou, Zhi & Ou, Jinping. 2004b. Interface strain transfer mechanism and error modification for adhered FBG strain sensor. *Fourth Asia-Pacific Conference Fundamental Problems of Opto-and Microelectronics, 13-16, September 2004, Khabarovsk, Russia, Laser press*(accepted by SPIE): 265-274.

Li, Jilong. Zhou, Zhi & Ou, Jinping. 2005. Interface Transferring Mechanism and Error Modification of Embedded FBG Strain Sensor Based on Creep Part I: Linear Viscoelasticity. *Smart Structures & materials/NDE Joint Conference Sensors and Smart Structures Technologies for Civil, Mechanical, and Aerospace Systems, 6-10 March 2005, Town and Country Resort & Convention Center, San Diego, California, USA*, SPIE number 5765-117, *Proc. SPIE Vol. 5765*

McClure, G. & Mohammadi, Y. 1995. Compression Creep of Pultruded E-Glass-Reinforced-Plastic Angles. *Journal of Materials in Civil Engineering, ASCE* 7(4): 269-276.

Nanni, A. Yang, C. C. Pan, K. et al. 1991. Fiber-optic sensors for concrete Strain/Stress Measurement. *ACI materials Journal* 88(3): 257-264.

Ou, Jinping. Zhou, Zhi & Wu Zhanjun. 2003. The sensing properties and practical application in civil infrastructures of optical FBGs. *SPIE* 5129.

Patrick, X. W. & Zou. 2003. Long-term properties and transfer longs of fiber-reinforced polymers. *Journal of Composites for Construction* 2:10-19.

Scott, D. & Zureick, A. 1998 Compression Creep of a Pultruded E-Glass/Vinylester Composite. *Composites Science and Technology*, *Elsevier* 58:1361-1369.

Shao, Y. & Shanmugam, J. 2004. Deflection Creep of Pultruded Composite Sheet Piling. *Journal of Composites for Construction, ASCE* 8(5): 471-478.

Task Committee. 1984. On Design of the Structural Plastics Research Council of the Technical Council on Research of the American Society of Civil Engineers. *Structural Plastics Design Manual. ASCE manuals and reports on engineering practice* No. 63, ASCE, New York: 199-210

Zhou, Zhi. Wu, Zhanjun. & Ou Jinping. 2002a. Technique and Application of In-situ Monitoring for Concrete Structures with FBG Sensors. *Pacific Science Review.* Far East Technical University of Russian, Vlasivostok, Vol.4.

Zhou, Zhi. Zhao, Xuefeng & Ou, Jinping. 2002b. A coating technique with steel capillary for FBG and its sensing properties. *Chinese Laser* 29 (12): 1089-1092.

Zhou, Zhi. 2003. Optical Fiber smart Bragg Grating Sensors and Intelligent Monitoring Systems of Civil Infrastructures. *PhD Dissertation, Harbin Institute of Technology, Harbin, China.*

Zhou, Zhi. Wu, Zhanjun. & Ou Jinping. 2003. Smart Monitoring Technique of Concrete Structures Based on Optical Fiber Bragg Grating Sensors. *Function Materials* 34 (3): 344-348.